

Chapter 4

Thiolate Hydrogen Bonding Mutants: Kinetics

4.1 Abstract

The heme-thiolate enzymes cytochromes P450, chloroperoxidase, and nitric oxide synthase all activate dioxygen to oxidize substrates. In each of these enzymes, there is a conserved hydrogen bonding network around the proximal thiolate ligand. These hydrogen bond donors come predominantly from backbone amide groups and help to tune the electronics of the heme center. However, in nitric oxide synthase one of these three hydrogen-bond donating groups comes from the side chain of a tryptophan residue, making nitric oxide synthases unique. Three mutant forms of the nitric oxide synthase from *Geobacillus stearothermophilus* were expressed in *E. coli*. These mutants each have a single point mutation, converting this native tryptophan residue to a histidine, phenylalanine, or tyrosine. The reactivity of each the wild type enzyme and the three new mutants were tested using stopped-flow mixing coupled with UV-visible absorption spectroscopy and the Griess Assay. Autoxidation rates measured by stopped-flow suggest that the Tyr and Phe mutants do indeed have significantly more negative reduction potentials, but that the His mutant is particularly slow to oxidize. The Griess Assays showed that all four enzymes produce nitrite in solution, when provided with substrate, cofactor, and hydrogen peroxide (as a source of reducing equivalents). In single turnover experiments, however, only three of the four enzymes showed evidence of ferric-NO production. The His mutant showed no intermediate absorbance near 440 nm (which would be indicative of ferric-NO formation), suggesting that it releases NO^- rather than the radical species $\text{NO}\cdot$.

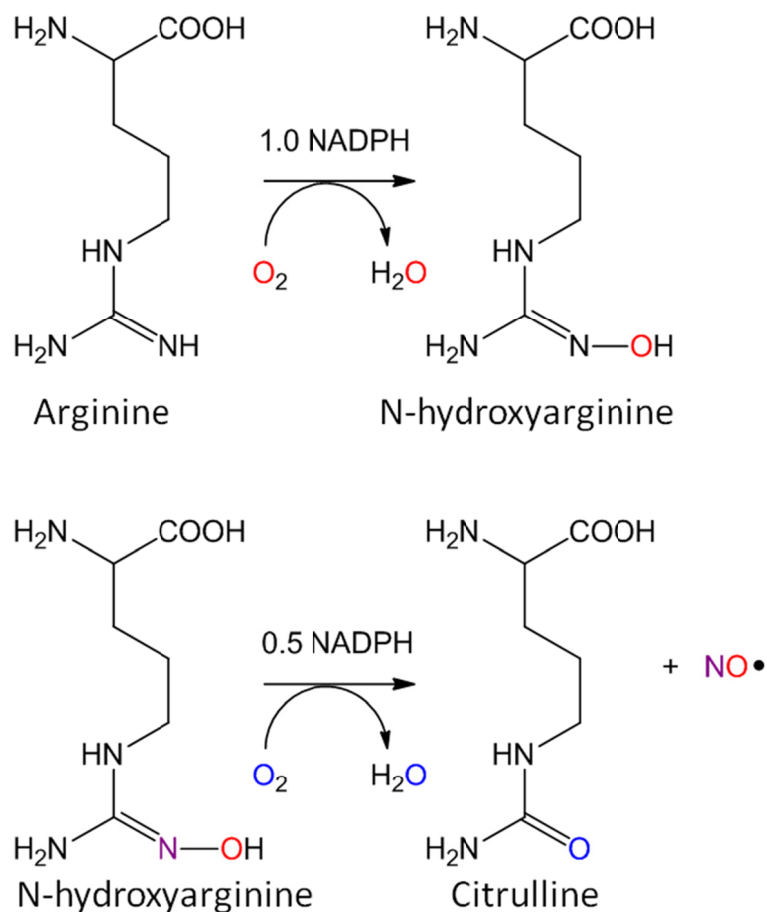
4.2 Introduction

As stated previously, nitric oxide synthases are the family of enzymes responsible for production of the signaling molecule NO.¹⁻² It was shown by Moncado³ that the active biological signaling molecule is in fact NO· and not any other NO_x species. It is this molecule that induces relaxation of the cells lining the walls of blood vessels, thus regulating blood flow in mammals. Since that time, the field of NO signaling has grown rapidly and it is now known that nitric oxide is also involved in neurotransmission, the immune response, and apoptosis.^{1-2, 4}

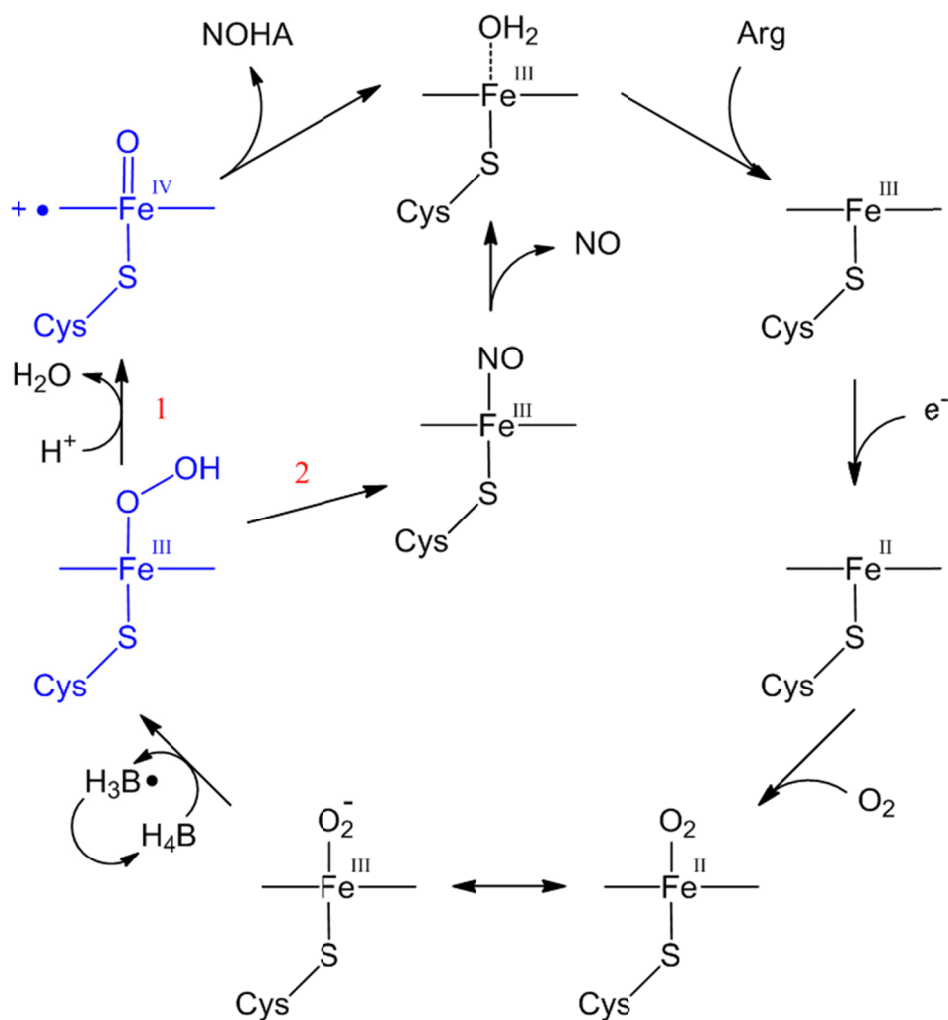
This family of enzymes makes NO from arginine (Arg) in two turnovers, through the enzyme-bound intermediate N-hydroxyarginine (NOHA) (**Scheme 4.1**).⁵⁻⁶ Much of what is known about its catalytic cycle is similar to the well-studied cytochrome P450.⁷⁻⁸ The observed intermediates (as well as probable intermediates in blue) are shown in the cycle in **Scheme 4.2**.

The resting state of the enzyme is a ferric heme with a loosely coordinated water molecule.⁹ This is displaced sterically when substrate binds within the enzyme, forcing a five-coordinate complex and shifting the iron to the high spin state. The heme is then reduced (in mammalian systems, reducing equivalents come from a dedicated reductase domain fused into the same polypeptide chain) to form a ferrous-heme complex. Reduced iron species readily bind dioxygen in biological systems. The ferric-oxy species (or ferric-superoxo depending on assignment of electrons, as shown by the equilibrium at the bottom of the cycle in **Scheme 4.2**) in cytochrome P450 is reduced by another electron from the reductase domain. NOS is unique in that this electron comes from a redox active cofactor called tetrahydrobiopterin (pterin) (**Scheme 4.3**). After this event, the next

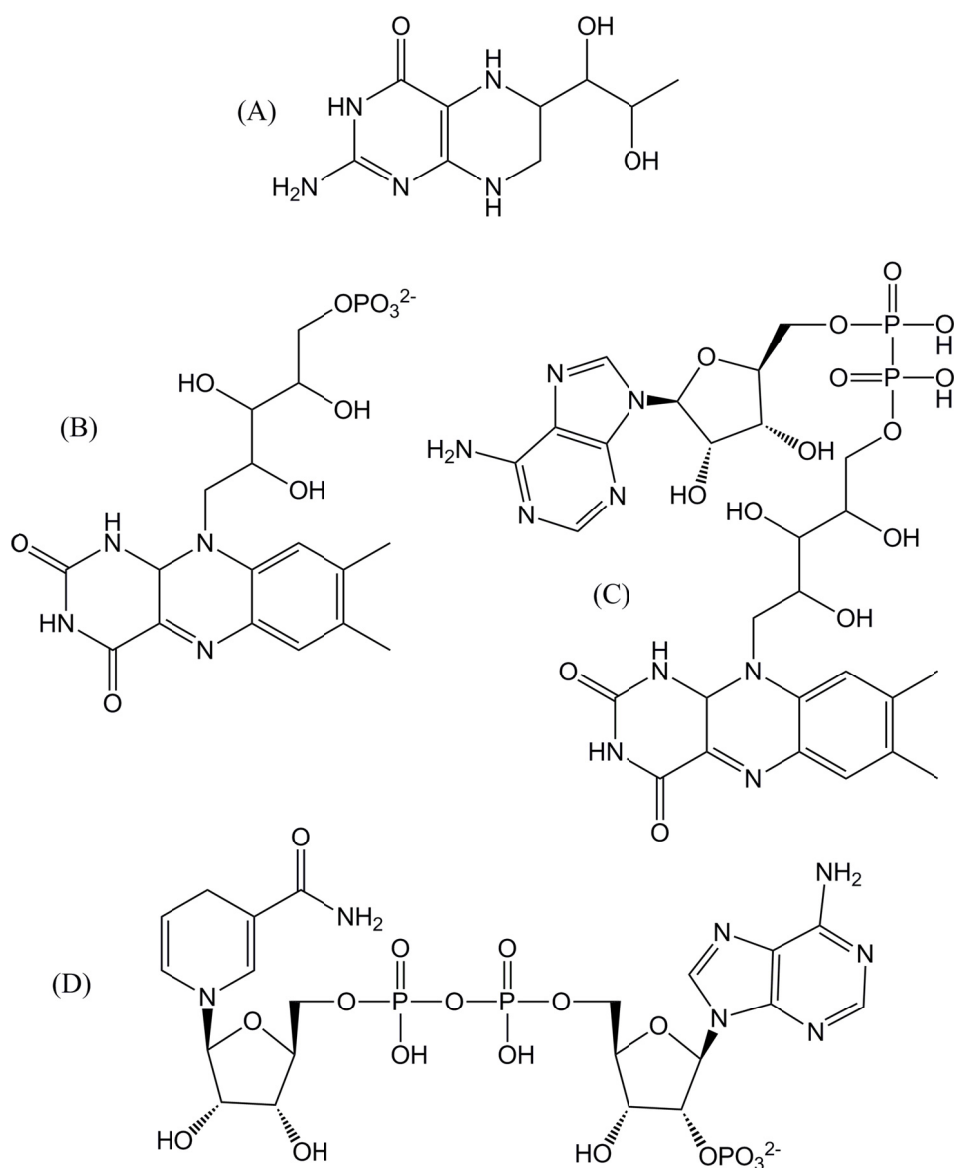
observed species is either the resting state of the enzyme (in the first turnover) or the ferric-NO complex (second turnover). The ferric-NO complex slowly releases NO to regenerate the resting state. The species responsible for actively oxidizing the substrate has not been definitively identified.¹⁰



Scheme 4.1. Production of NO and citrulline by nitric oxide synthases from the starting material arginine through the enzyme-bound intermediate N-hydroxyarginine.



Scheme 4.2. The putative reaction mechanism of nitric oxide synthases: (1) first turnover, Arg hydroxylation, (2) second turnover, NO production.

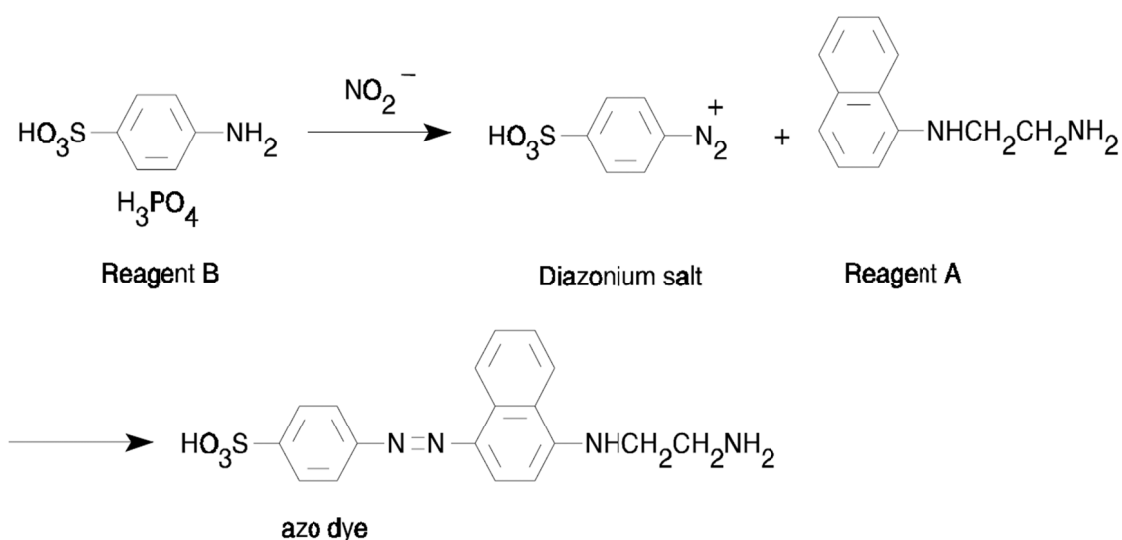


Scheme 4.3. Cofactors involved in electron transfer in NOS: (A) tetrahydrobiopterin, (B) FMN, (C) FAD, and (D) NADPH.¹¹ B–D all bind in the reductase domain of mammalian enzymes rather than in the oxygenase domain common to all species.

The mechanism of NOS has been studied extensively in order to elucidate the details of NO production.¹²⁻¹³ The most useful technique to date has been stopped-flow mixing coupled with UV-visible absorption spectroscopy. With UV-vis, one can follow the ligation and oxidation state of the heme center. Coupling this with a rapid mixing

setup allows researchers to follow the heme spectroscopically as it turns over and produces nitric oxide.¹⁴

In stopped-flow experiments, catalysis is initiated through careful mixing of the enzyme with a reactant. In the case of NOS, a degassed solution of the reduced form of the enzyme, with tetrahydrobiopterin and the enzyme-bound intermediate NOHA fully loaded, is mixed with aerated buffer to introduce oxygen. Oxygen is the last ingredient needed to initiate turnover. However, because no extra reductant is present to re-reduce the heme and pterin after the cycle, only a single turnover can occur. When monitored by UV-vis, these stopped-flow mixing experiments allow researchers to watch NOS at work as it produces NO. Using this technique, researchers have characterized the ferrous-oxy and ferric-NO complexes of the enzyme, but other intermediates react too quickly to be detected.² Observation of the ferric-NO complex during turnover is used as a spectroscopic handle in order to show that an enzyme does in fact produce NO.



Scheme 4.4. Reaction scheme for the Griess Assay.

Another common method used to characterize NO production is called a Griess Assay. In aqueous solution, nitric oxide rapidly reacts to form nitrite and other NO_x species.⁶ Reagents were developed to react specifically with nitrite, again in aqueous solution, in order to spectroscopically characterize *in vivo* NO production (**Scheme 4.4**).¹⁵ Reagent B reacts with NO₂⁻ (nitrite) to form a diazonium salt, which then reacts with Reagent A to form an azo dye with an intense visible absorption band at 540 nm. The molar absorptivity of this band is known so it can be used to determine the amount of nitrite in solution.

Both stopped-flow UV-vis spectroscopy and the Griess Assay were used to investigate the kinetics and reactivity of a series of mutant enzymes of nitric oxide synthase. The NOS used in these studies is that from *Geobacillus stearothermophilus* (gsNOS).¹⁶⁻¹⁷ This particular organism is a bacterial thermophile, and therefore its enzymes have been optimized to function at elevated temperatures. This adds to the stability of their fold,¹⁵ a notorious problem for the mammalian nitric oxide synthases. This enzyme, gsNOS, has a particularly stable ferrous-oxy intermediate. In the absence of substrate, rate constant for its decay is less than 0.1 s⁻¹. This has led to its use in other studies, such as the experiments conducted by Davydov and Hoffman which give the only evidence for both of the blue intermediates shown in **Scheme 4.2**.¹²⁻¹³

The mutants investigated in the studies presented here have been introduced previously (see Chapters 1 and 3, **Figure 4.1**). The role(s) of the proximal hydrogen bonding network involving the axial thiolate ligand were investigated. Three mutant enzymes, W70H, W70F, and W70Y, were expressed and their reactivity (along with the wild type enzyme) was investigated by stopped-flow UV-visible absorption spectroscopy

as well as through use of the Griess Assay. It was found that their autoxidation rates support the data from redox titrations (Chapter 3) and together suggest that the potential of W70H is slightly higher than wild type, while the potentials of W70F and W70Y are much more negative. The Griess Assay confirmed nitrite production in all four of the mutants, however with either significant de-coupling or a decreased rate in the W70F and W70Y mutants. The presence of a ferric-NO intermediate was confirmed using single turnover experiments in three of the four enzymes. Surprisingly, no evidence for this species was observed in the W70H mutant, suggesting production of NO^- rather than the radical NO.

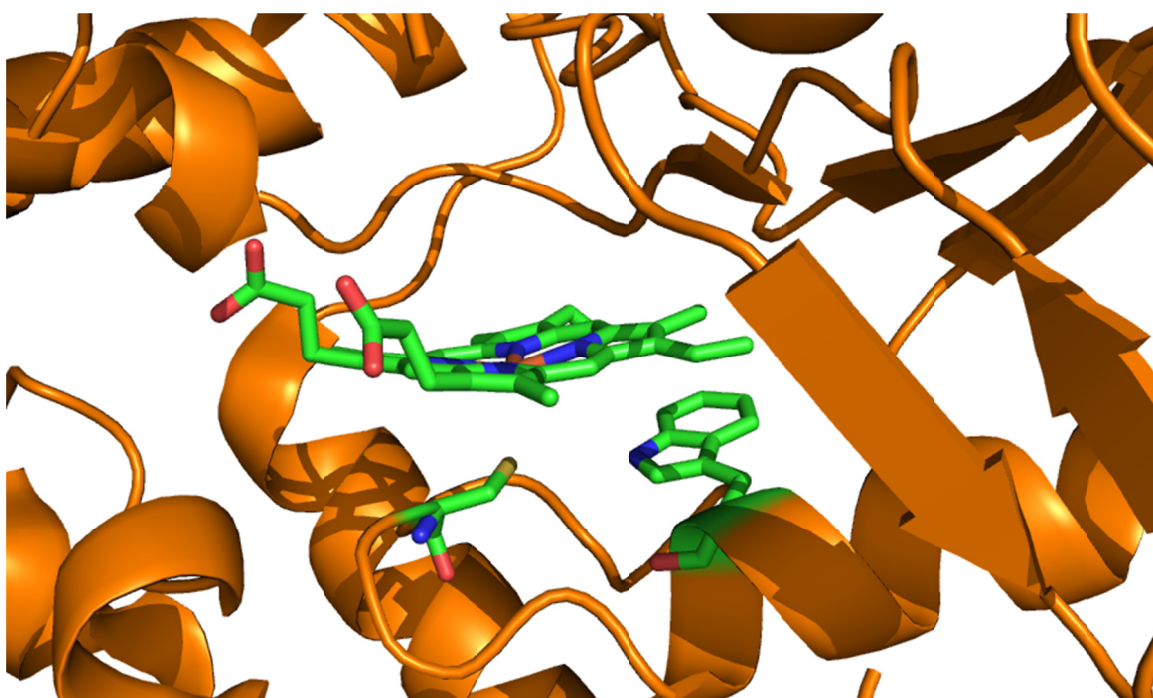


Figure 4.1. Close up of the heme center of gsNOS, with the axial thiolate and Trp70 highlighted in green (PDB file 2FLQ).

4.3 Materials and Methods

Sample Preparation

The plasmid for the nitric oxide synthase from *Geobacillus stearothermophilus* was a gift from the lab of Brian Crane. This enzyme was expressed as previously described by Sudhamsu and Crane with no significant deviations in procedure.¹⁵ The enzyme was overexpressed in *Escherichia coli* BL21 (DE3) cells. Cells were grown to an optical density of approximately 1.0–1.4 and induced by adding a solution containing iron(III) chloride, IPTG, and δ -aminolevulinic acid (Aldrich) to final concentrations of 125 mg/L, 100 μ M, and 50 mg/L, respectively, in milliQ water. The pETDuet vector (Novagen) coded for a C-terminal cleavable His₆-tag so samples were purified using metal affinity chromatography. (This vector also confers chloramphenicol resistance to the cells, so 34 μ g/mL of this antibiotic were added to all cultures in Luria broth.) The His₆-tag was then cleaved using bovine thrombin (Calbiochem). Both thrombin and the His-tag were removed using size exclusion chromatography. Sample purity and Soret band epsilon values were determined through use of the hemochromagen assay.

A QuikChange site-directed mutagenesis kit from Stratagene was used to make the desired mutations in the amino acid backbone. Primers were designed according to the guidelines outlined by the QuikChange kit manual. Unless otherwise noted, protein solutions were made in the following buffer: 50 mM Tris (2-amino-2-hydroxymethylpropane-1,3-diol), 150 mM NaCl, pH 7.5 (the same buffer used for size exclusion chromatography). Steady-state UV-visible spectra were collected on an Agilent HP 8452 diode array spectrophotometer.

Stopped Flow UV-Visible Spectroscopy

Samples were prepared anaerobically and transferred to an anaerobic tonometer with 1.5 equivalents of dithionite to scavenge any residual oxygen. Dithionite was used to scavenge oxygen from the stopped flow spectrophotometer (HiTech Scientific) syringes and excess dithionite was removed by repeated washing with anaerobic buffer. For autoxidation rates, samples of reduced protein (4–6 μM gsNOS) free of substrate and pterin cofactor were mixed with aerated buffer. Autoxidation rates were also measured in the presence of 2.5 mM Arg and 15 μM pterin. Protein samples for single turnover experiments (4–6 μM gsNOS loaded with, 60 μM H4B and 200 μM N-hydroxy-L-arginine) were rapidly mixed with air-saturated buffer. All experiments were conducted at 4 °C. The formation and release of NO in the single turnover experiments was monitored using a diode array detector and the rates fit globally using SpecFit32 (HiTech Scientific). Measured rates were independent of protein concentration under experimental conditions and all measurements were repeated at least six times before averaging.

Griess Assay

In order to quantify turnover in each of the enzymes, NO production was monitored using the Griess Assay. Reagents A and B were purchased from Cayman Chemicals. Solutions were made containing of 100 μL of 30 μM NOS and 1 mM arginine in 150 mM NaCl, 50 mM Tris buffer at pH 7.5. To these solutions, 2 μL of 1M H_2O_2 was added to a final concentration of 20 mM. The solution was allowed to react for three minutes before addition of Reagent B, which stops the reaction and denatures the protein. The sample must be allowed to sit for ten minutes before addition of Reagent A in order to allow formation of nitrite from aqueous nitric oxide. The UV-visible

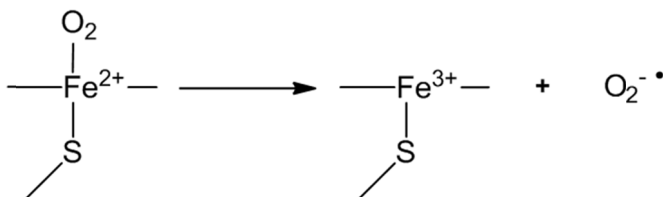
absorption spectrum is then recorded. Absorbance at 540 nm is related to the concentration of nitrite by the following equation (from Cayman Chemicals). All measurements were made in triplicate.

$$\text{Absorbance} = 0.030 + 0.029[\text{nitrite}] \quad (4.1)$$

4.4 Results and Discussion

Autoxidation Rates

The reactivity of each wild type gsNOS and three mutants (W70H, W70F, and W70Y) was studied by stopped-flow UV-visible spectroscopy. The reduced form of all heme-thiolate enzymes reacts quickly with dioxygen. Samples of approximately 5 μM NOS in Tris buffer were mixed in a 1:1 ratio with oxygenated buffer (air-saturated) and the regeneration of the ferric state was monitored. Given that this particular enzyme has such a long-lived ferrous-oxy species, the kinetics of each mutant's reactivity with dioxygen was investigated. It is unclear how this enzyme is tuned to produce such a stable complex and what purpose that may serve. Upon mixing with dioxygen, samples quickly form a ferrous-oxy species which then dissociates into the ferric form of the enzyme and a reduced superoxide species (**Scheme 4.5**). In the absence of substrate and pterin cofactor, clean formation of the ferrous-oxy species is not observed, only the transformation from ferrous enzyme to ferric enzyme.



Scheme 4.5. Reaction of oxygen with reduced gsNOS forms a ferrous-oxy complex, and then releases superoxide from the oxidized heme.

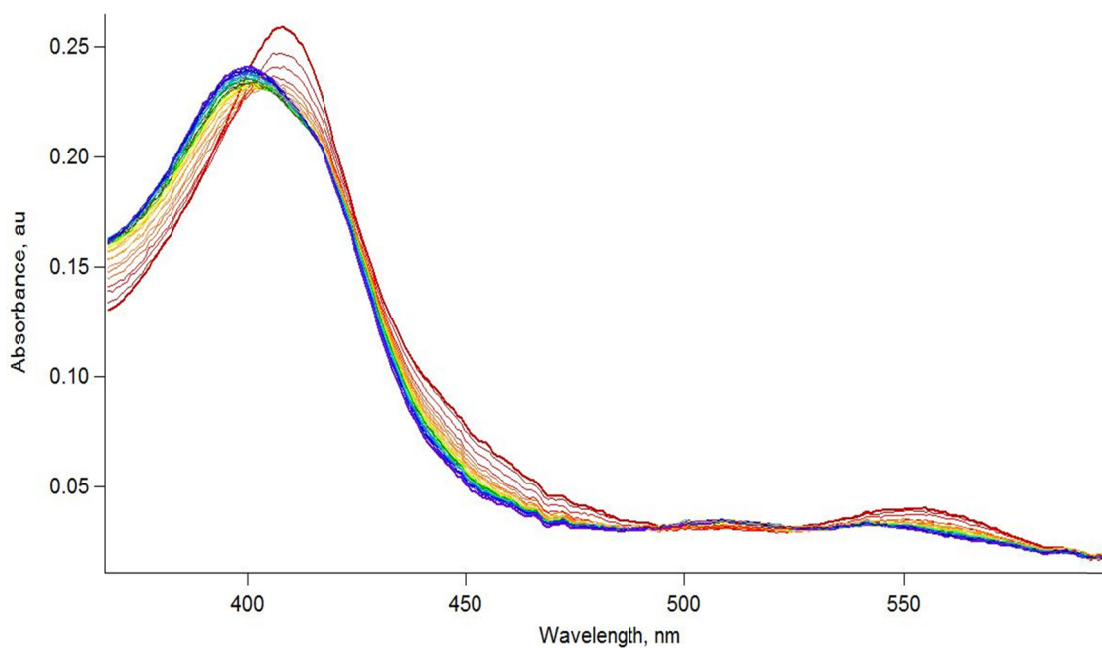


Figure 4.2. Oxidation of W70F upon rapid mixing of reduced enzyme with oxygenated buffer. Ferrous gsNOS (red trace) partially converts to the ferric heme over the course of 22.5 seconds. For full kinetics analysis, scans were collected out to 45 seconds to allow for full formation of the ferric species.

These three single point mutations at position 70 were found to have a large effect on autoxidation rates. For the wild type enzyme, scans of 225 seconds were required in order to catch the full transformation to the oxidized resting state. The ferrous state of the Tyr mutant reacts much more quickly, taking only 9 seconds to completely oxidize. The Phe and Tyr mutants have higher rate constants than wild type for autoxidation by factors of 2.5 and 6, respectively. Interestingly, the His mutant has a rate constant that is one full order of magnitude lower. This is certainly caused by altered electronics of the heme center, but the exact reason for this is unknown. While the reduction potential of this enzyme was reported to be significantly higher than the wild type in mammalian inducible NOS by another group,¹⁸ our data suggest that the potential of this enzyme is

not as elevated relative to wild type (Chapter 3). Another factor may be the π -stacking of the tryptophan residue with the porphyrin ring, of which histidine is incapable.

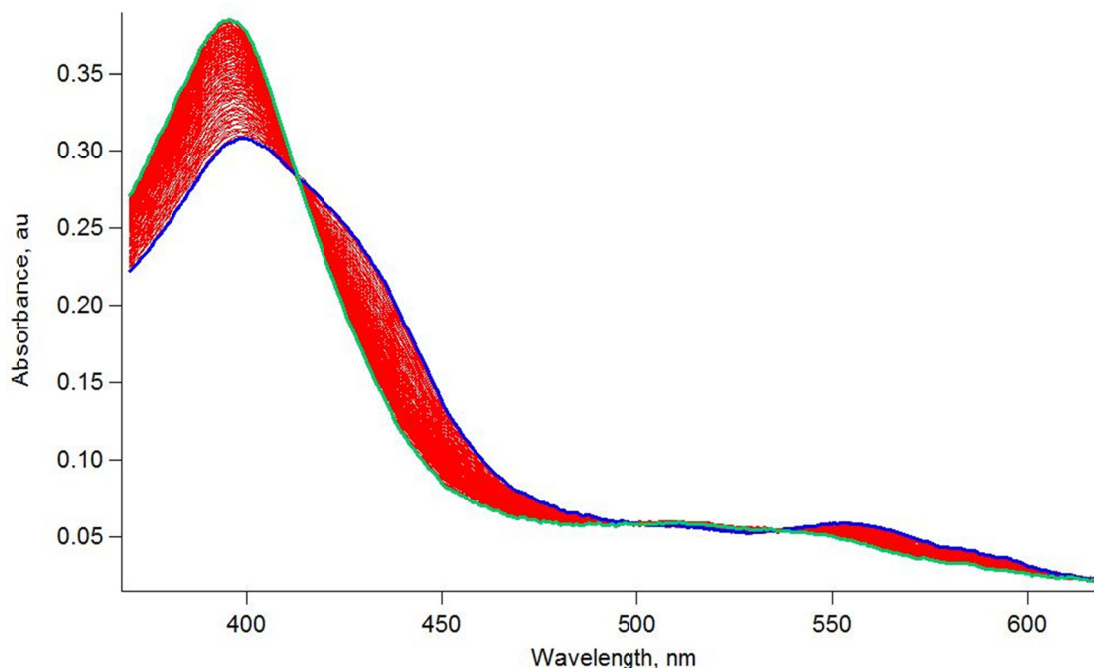


Figure 4.3. Oxidation of W70H in the presence of arginine and tetrahydrobiopterin. Initial scan upon mixing (blue trace) before formation of the ferric state (green).

It has been shown previously that both substrate and tetrahydrobiopterin cofactor contribute to the decay of the ferrous-oxy species and speed formation of the resting state. This is presumably due to the ability of the enzyme to now undergo catalysis, as all necessary ingredients are present. Faster scans show clean formation of the ferrous-oxy species, rather than catching only a shoulder (blue trace, **Figure 4.3**) before conversion to the ferric state. However, longer scanning times are required to observe full formation of the ferric state. The rate constant of interest is that of the oxidation to ferric, so longer scans were used for kinetics analysis. All data were fit to a three-state model, where the ferrous-oxy is formed very rapidly, followed by conversion to the ferric enzyme.

Calculated rate constants for conversion of the ferrous-oxy intermediate to the ferric resting state (from SpecFit software) are shown in **Table 4.1**.

Table 4.1. Rate constants for oxidation of each mutant enzyme, with and without substrate/cofactor.

| Sample | Oxidation rate, s^{-1} | With substrate, s^{-1} |
|--------|--------------------------|--------------------------|
| WT | 0.096 | 0.51 |
| His | 0.0098 | 0.19 |
| Phe | 0.23 | 2.6 |
| Tyr | 0.62 | 4.3 |

The effect of the presence of arginine and the pterin cofactor is apparent from **Table 4.1**. The rate constant for oxidation of the wild type enzyme is increased by the smallest amount among the four enzymes, a factor of approximately 5, while the W70H mutant oxidizes faster in the presence of these two additional substances by a factor of nearly 20. This is a remarkable increase. The data show that the ferrous-oxy species of the W70H mutant is much more stable than the others, by an order of magnitude or more, but this effect is lessened under catalytic conditions where reactivity of the enzyme toward substrate dominates the kinetics rather than simple oxidation of the iron center.

Assuming that all four samples interact with dioxygen in the same manner, the rates of autoxidation of the heme should correlate with the reduction potentials. This is consistent with results from Chapter 3 showing that the reduction potential of the Phe and Tyr mutants are significantly more negative than wild type and W70H. The presence of this single, long hydrogen bonding interaction brings the reduction potential more

positive. The potential of the W70F and W70Y mutants is most likely too negative to allow reduction by a reductase enzyme *in vivo*.

Griess Assay

The function of nitric oxide synthases is to produce nitric oxide. This radical species reacts rapidly in aqueous solution, making it difficult to quantify NO production. One of the compounds that NO forms in buffered solutions is NO_2^- , nitrite. A colorimetric assay for this species has been developed and patented, allowing for the facile determination of nitrite concentrations in solution. This should be proportional to the amount of NO originally formed by the enzyme.

Table 4.2. Nitrite production rates by gsNOS mutants.

| Sample | NO_2^- production, $\text{heme}^{-1} \text{ min}^{-1} \times 100$ |
|--------|--|
| WT | 10.7 ± 0.6 |
| His | 13.9 ± 0.7 |
| Phe | 4.3 ± 0.1 |
| Tyr | 3.4 ± 0.1 |

With wild type as a benchmark, W70H shows increased nitrite production while W70F and W70Y show a marked decrease in production. This decrease could be caused by any of several things. First, if a mutant produces NO at a decreased rate, this would lead to decreased consumption of reducing equivalents from the hydrogen peroxide and less nitrite in the solution. Alternatively, if the electronics of the system have been unbalanced, a decrease in quantity of nitrite could mean similar or even increased consumption of reducing equivalents, but with uncoupling of this from NO production. The enzyme would instead release superoxide or other compounds, or even oxidize parts

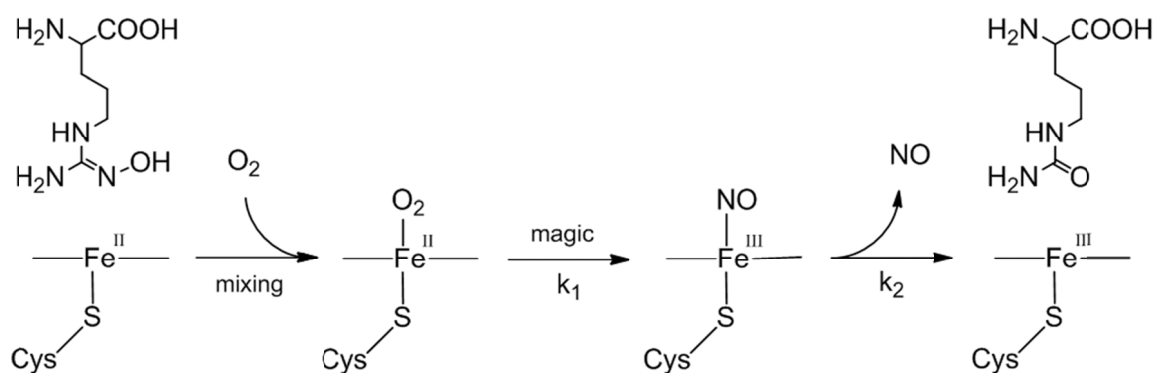
of the protein itself leading to degradation. Unfortunately, the Griess Assay can tell us only the amount of nitrite in any given aqueous solution.

Hydrogen peroxide has sufficient driving force to reduce all four of these protein samples (-680 mV). Upon mixture with the enzyme, a ferric-hydroperoxo species is formed (the first complex in blue in **Scheme 4.2**). Due to their more negative reduction potentials, the Tyr and Phe mutant enzymes autoxidize very rapidly. This means that their rate of consumption of reducing equivalents should be equal or even increased compared with wild type regardless of catalytic activity. Without this conserved hydrogen bond, the hydroperoxo complex may react too quickly to release reactive oxygen species and the ferric enzyme without reacting with the substrate. Alternatively, with a better donating thiolate ligand, O-O bond cleavage may occur incredibly rapidly. This would form Compound I (second species in blue in **Scheme 4.2**) and facilitate the first turnover, but perhaps not provide enough time for the ferric-hydroperoxo to react with NOHA in the second turnover, preventing NO formation. Catalysis using hydrogen peroxide as reductant and the source of dioxygen has been shown to produce cyano-ornithine in mammalian inducible NOS rather than citrulline (and NO).¹⁹

Single Turnover Experiments

To observe turnover of the enzyme, stopped-flow mixing was employed coupled with UV-visible absorption spectroscopy for detection of intermediates. The resting state of the enzyme, with substrate and cofactor bound, has a Soret band with a maximum absorption at 396 nm. The position of this band is very consistent across isoforms, while the substrate and cofactor-free forms can vary from 400 (gsNOS)¹⁵ to 421 nm (mammalian iNOS).¹⁹⁻²⁰ The ferrous-oxy complex, formed immediately after mixing the

enzyme with aerated buffer, has a maximum absorption around 428–430 nm, depending on isoform.¹⁴ This is the last intermediate observed before the formation of the NO-bound ferric heme complex, with a maximum absorption near 440 nm.²¹ This releases NO to regenerate the resting state of the enzyme. Each of these species can be observed by stopped-flow and resolved by UV-vis, allowing researchers to literally watch NOS as it functions. This reaction scheme is shown in **Scheme 4.6**, detailing the steps from the ferrous enzyme introduced in one syringe, to the production of citrulline and NO. Unfortunately, the active oxidant (Compound I or the hydroperoxo-heme complex) reacts much too quickly to build up to any appreciable level and be observable by this technique, thus k_1 is ultimately a mixture of several elementary steps leading to ferric-NO formation.²² Compound I has only been cleanly generated and characterized recently by stopped-flow in a thermophilic cytochrome P450.²³



Scheme 4.6. Reaction of reduced NOS with oxygenated buffer, provided that tetrahydrobiopterin is present, showing the release of NO.

For fitting purposes, a three-state model is used, beginning with the ferrous-oxy species and finishing with formation of the resting state through another intermediate (which correlates with the ferric-NO complex). These correspond to the second, third, and fourth complex shown in **Scheme 4.6**, with the software fitting two rate constants, k_1

and k_2 . Despite k_1 incorporating many elementary steps, this model for fitting the kinetics data fits all spectra well using the SpecFit software.

In all cases the first trace shows the five-coordinate ferrous species, prior to formation of the ferrous-oxy. This arises due to the use of excess reductant, which is necessary to ensure that the enzyme remains fully reduced in the syringe. The reductant, sodium dithionite, reacts several orders of magnitude more rapidly with oxygen than the enzyme.²⁴ Thus, the small excess of dithionite (less than 1 equivalent of the enzyme so as not to greatly alter the initial concentration of oxygen in solution) will react completely before the other chemical reactions occur. Typical traces for the wild type enzyme are shown in **Figure 4.4** below. The ferrous complex can be seen in the first (and only the first) trace, red. The second trace, in green, corresponds well with formation of the ferrous-oxy complex. This formation is complete before the second trace can be collected, thus the rate is too fast to be calculated accurately from these data. For all kinetics analyses the first spectrum is discarded, as this is the only spectrum where the ferrous-unligated complex is visible. In every case the spectra first red-shift (relative to the five-coordinate ferrous starting material) before blue shifting to the ferric species.

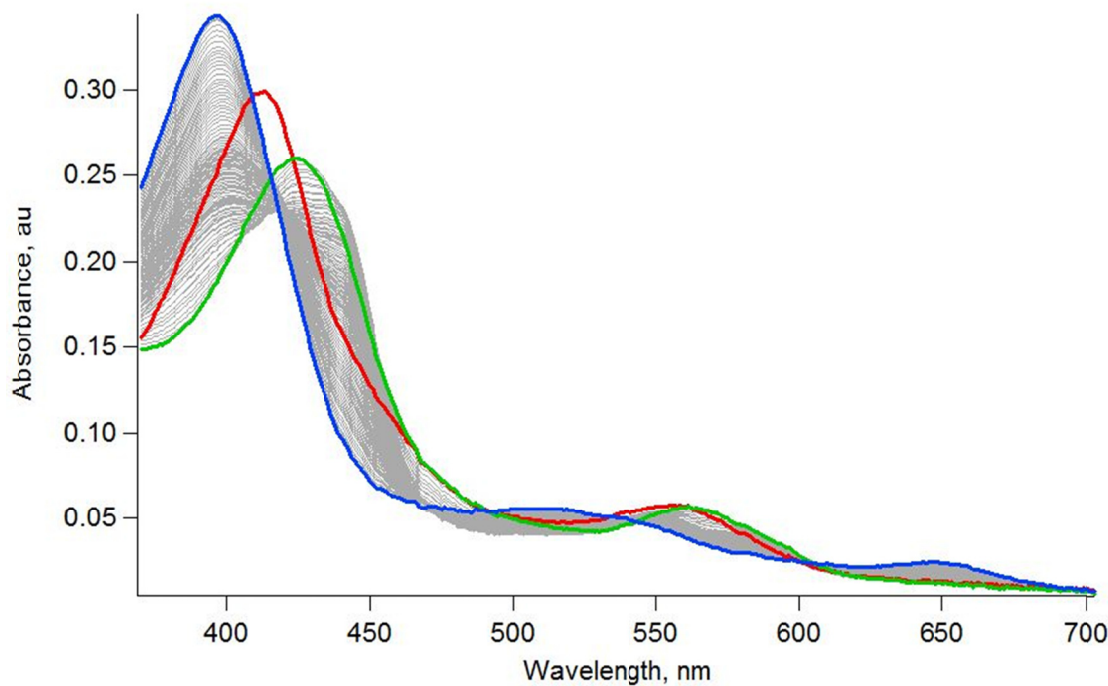


Figure 4.4 Single turnover reaction of wild type gsNOS. Five-coordinate ferrous (red), ferrous-oxy (green), and the resting ferric state (blue).

The spectra shown above are consistent with stopped-flow data collected on other nitric oxide synthases, such as for the NOSs from mammalian macrophages (iNOS) and *Bacillus subtilis*.^{14, 25} One key feature is the further red-shift of the Soret band beyond the ferrous-oxy complex (seen in gray just to the right of the maximum absorbance for the green trace). The Soret band for the pure ferric-NO complex has a maximum absorbance at 440–442 nm, depending on isoform.¹⁴ The formation of this complex can be seen more clearly for the W70Y mutant, shown in **Figure 4.5**.

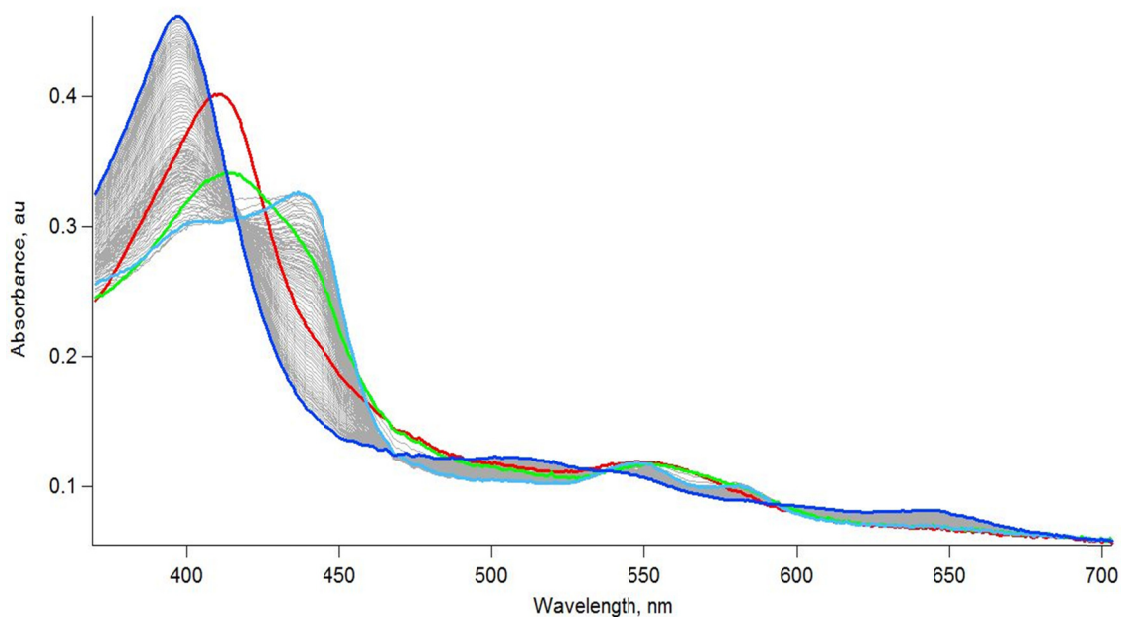


Figure 4.5. Single turnover reactions of W70Y gsNOS. In these traces, the formation of the ferric-NO complex can be seen most clearly in this mutant. These are also representative of the W70F mutant.

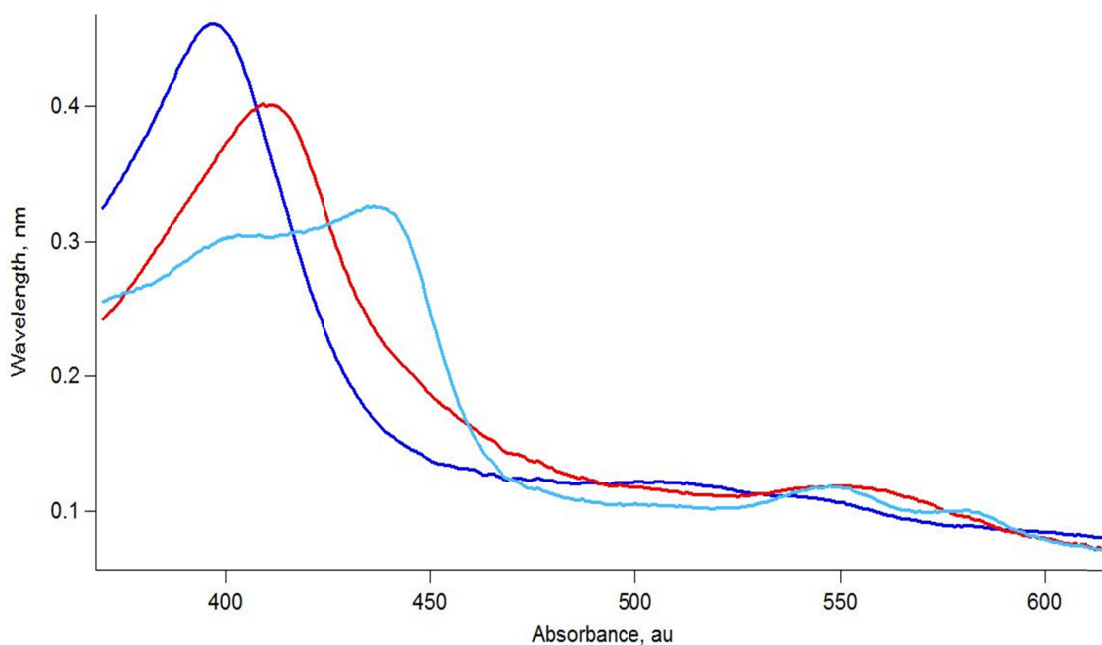


Figure 4.6. The spectrum generated for intermediate B (light blue) with the ferrous (red) and ferric (dark blue) spectra for reference. The light blue trace clearly shows a mixture of two species by Soret bands, the ferric-NO complex, with a maximum absorbance at 438 nm in this spectrum, and the ferric resting state of the enzyme, with a maximum absorbance of 398 nm.

While clear evidence is seen for the formation of the ferric-NO complex for the wild type enzyme and the W70F and W70Y mutants, this is absent in the W70H mutant. Traces collected for the histidine mutant are shown in **Figure 4.7**. The spectrum with the Soret band farthest to the red is that of the second trace, with a peak at 430 nm and broad Q-bands corresponding to the ferrous-oxy complex. At no point do any of the traces shift further to the red and the fitting software is unable to extract any intermediate with a spectrum with even a shoulder near 440 nm. No evidence could be found to support the formation of a ferric-NO species in this particular mutant NOS.

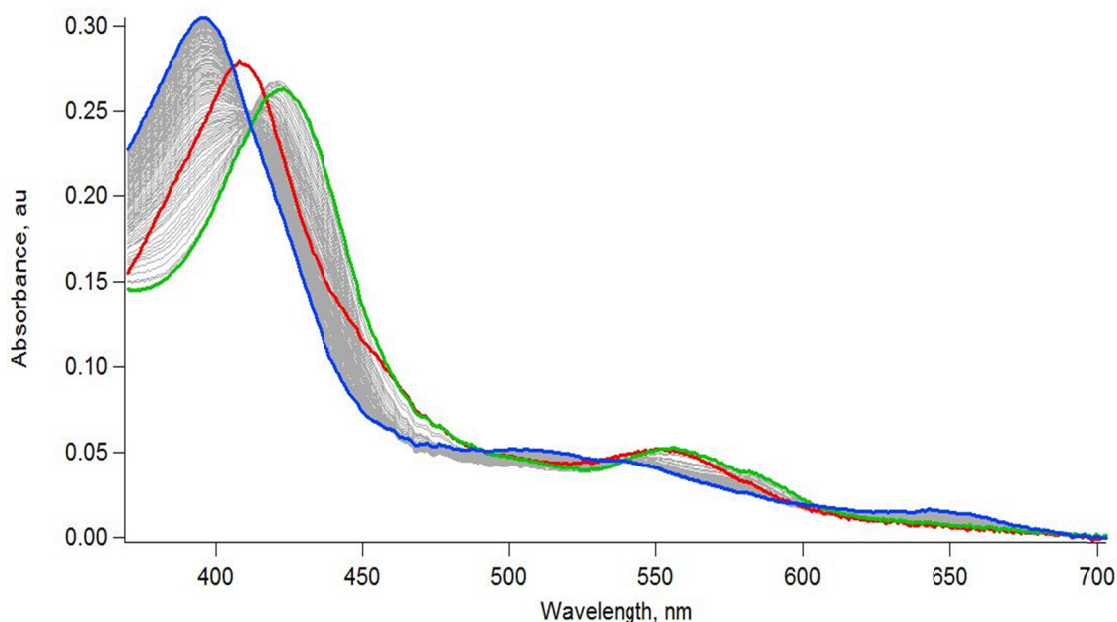


Figure 4.7. Single turnover reactions of W70H gsNOS. The second trace, green, shows clear formation of the ferrous-oxy complex, but no further red-shift of the spectra is seen.

It can be concluded from stopped-flow UV-vis data that the W70H mutant does not form a ferric-NO complex. Spectra look nearly identical to those collected with Arg and pterin, probing the oxidation rate in the first turnover but with an oxidation rate of 0.07 rather than 0.2. (This complex is observed by stopped-flow/UV-vis in all other NOS enzymes reported to date.) From the Griess Assay, it was shown that this enzyme releases

some NO_x at a rate actually increased relative to wild type. These data together suggest that the W70H mutant enzyme does not release $\text{NO}\cdot$ but rather NO^- from the heme center. The other three enzymes, however, clearly form ferric-NO complexes, as observed by stopped-flow.

4.5 Conclusions

Stopped-flow coupled with UV-visible spectroscopy was employed to characterize wild type gsNOS and these three new mutant enzymes. It was shown that their autoxidation rates correlate with reduction potential data discussed in Chapter 3. The histidine mutant has an elevated reduction potential and the slowest autoxidation rate relative to the other three. The wild type is more negative by approximately 20 mV with a potential of -362 mV vs. NHE. This reduction potential is similar to that of mammalian inducible NOS, but these two are then more negative than other NOS enzymes by 100 mV.²⁶ The reason for this behavior in gsNOS is unknown, but in iNOS the presence of the substrate sterically excludes a water molecule that coordinates the heme and this binding event shifts the reduction potential into the normal range for NOSs. The two mutants lacking this conserved hydrogen bond, W70F and W70Y, have significantly more negative potentials and were found to have very fast rate constants for autoxidation, consistent with more negative potentials.

The production of NO_x species of all four enzymes was characterized by the Griess Assay. The wild type produces nitrogen oxide species at a rate similar to other NOSs. The W70H mutant has an elevated rate of NO_x release/formation. The two mutants without this hydrogen bond have significantly decreased rates of NO_x

production. Clearly this hydrogen bond plays a role in the rate of NO release from the enzyme or the speed with which it is formed (as all four should react sufficiently rapidly with hydrogen peroxide for reduction not to be a factor).

Finally, stopped-flow was once again employed in order to determine if the Griess Assay was indeed detecting NO \cdot or rather NO $^-$ which are indistinguishable by that method. The ferric-NO complex, the immediate precursor to the nitric oxide product, was observed for three of the four enzymes. Interestingly, this could not be observed for the W70H mutant. This mutant most likely releases NO $^-$.

The conserved proximal hydrogen bond donating group found near the axial thiolate ligand in all nitric oxide synthases plays a key role in tuning the electronics of the active site. This is a uniquely long hydrogen bonding interaction between this tryptophan and the thiolate, at just 3.7 Å. Without this interaction, the enzyme is still capable of producing NO, as found for both the W70F and W70Y mutants by single turnover experiments. Their reduction potentials, however, are incredibly negative and most likely fall far below the biologically relevant window. The replacement of this tryptophan with a histidine results in an enzyme with a more elevated potential, however it cannot release NO radical. The histidine residue, lacking the aryl ring, most likely cannot π -stack with the porphyrin ring, giving it more flexibility. This may allow it to move closer to the thiolate to improve this hydrogen bonding interaction. If this interaction is too strong, NO $^-$ is released.

In the second turnover of the catalytic cycle, an electron from the heme center must be shuttled back into the tetrahydrobiopterin cofactor to re-reduce it. The potentials of both the heme and the pterin must be tuned perfectly to allow forward electron transfer

into the ferrous-oxy complex followed by back electron transfer into the pterin. This back electron transfer allows release of $\text{NO}\cdot$ and not NO^- .²⁷ If the potential of the heme center is too high, this back electron transfer cannot occur, preventing $\text{NO}\cdot$ release. Thus, the hydrogen bonding interaction is necessary for tuning the reduction potential high enough for the reduction of the heme by a reductase domain/enzyme. However, when too strong, the potential is tuned too high to send an electron back into the pterin after catalysis, which is necessary for formation of the product NO .

4.6 References

1. Marletta, M. A. (1993) Nitric-oxide synthase structure and mechanism, *J. Biol. Chem.* 268, 12231.
2. Stuehr, D. J., Santolini, J., Wang, Z. Q., Wei, C. C., and Adak, S. (2004) Update on mechanism and catalytic regulation in the no synthases, *J. Biol. Chem.* 279, 36167.
3. Palmer, R. M. J., Ferrige, A. G., and Moncada, S. (1987) Nitric-oxide release accounts for the biological-activity of endothelium-derived relaxing factor, *Nature* 327, 524.
4. Alderton, W. K., Cooper, C. E., and Knowles, R. G. (2001) Nitric oxide synthases: Structure, function and inhibition, *Biochem. J.* 357, 593.
5. Griffith, O. W., and Stuehr, D. J. (1995) Nitric oxide synthases: Properties and catalytic mechanism, *Annu. Rev. Physiol.* 57, 707.
6. Groves, J. T., and Wang, C. C.-Y. (2000) Nitric oxide synthase: Models and mechanisms, *Curr. Opin. Chem. Biol.* 4, 687.
7. Sono, M., Stuehr, D. J., Ikedasaito, M., and Dawson, J. H. (1995) Identification of nitric-oxide synthase as a thiolate-ligated heme protein using magnetic circular-dichroism spectroscopy - comparison with cytochrome p-450-cam and chloroperoxidase, *J. Biol. Chem.* 270, 19943.
8. Sono, M., Roach, M. P., Coulter, E. D., and Dawson, J. H. (1996) Heme-containing oxygenases, *Chem. Rev.* 96, 2841.
9. Dawson, J. H., and Sono, M. (1987) Cytochrome.P-450 and chloroperoxidase - thiolate-ligated heme enzymes - spectroscopic determination of their active-site structures and mechanistic implications of thiolate ligation, *Chem. Rev.* 87, 1255.
10. Martin, N. I., Woodward, J. J., Winter, M. B., Beeson, W. T., and Marletta, M. A. (2007) Design and synthesis of c5 methylated l-arginine analogues as active site probes for nitric oxide synthase, *J. Am. Chem. Soc.* 129, 12563.
11. Mowat, C. G., Gazur, B., Campbell, L. P., and Chapman, S. K. (2010) Flavin-containing heme enzymes, *Arch. Biochem. Biophys.* 493, 37.
12. Davydov, R., Ledbetter-Rogers, A., Martásek, P., Larukhin, M., Sono, M., Dawson, J. H., Masters, B. S. S., and Hoffman, B. M. (2002) Epr and endor characterization of intermediates in the cryoreduced oxy-nitric oxide synthase heme domain with bound l-arginine or n^g-hydroxyarginine, *Biochemistry* 41, 10375.
13. Davydov, R., Sudhamsu, J., Lees, N. S., Crane, B. R., and Hoffman, B. M. (2009) Epr and endor characterization of the reactive intermediates in the generation of no by cryoreduced oxy-nitric oxide synthase from geobacillus stearothermophilus, *J. Am. Chem. Soc.* 131, 14493.
14. Wei, C. C., Wang, Z. Q., and Stuehr, D. J. (2002) Nitric oxide synthase: Use of stopped-flow spectroscopy and rapid-quench methods in single-turnover conditions to examine formation and reactions of heme-o-2 intermediate in early catalysis, In *Enzyme kinetics and mechanism, pt f: Detection and characterization of enzyme reaction intermediates*, pp 320, Academic Press Inc, San Diego.

15. Sudhamsu, J., and Crane, B. R. (2006) Structure and reactivity of a thermostable prokaryotic nitric-oxide synthase that forms a long-lived oxy-heme complex, *J. Biol. Chem.* *281*, 9623.
16. Kabir, M., Sudhamsu, J., Crane, B. R., Yeh, S. R., and Rousseau, D. L. (2008) Substrate-ligand interactions in geobacillus stearothermophilus nitric oxide synthase, *Biochemistry* *47*, 12389.
17. Kinloch, R. D., Sono, M., Sudhamsu, J., Crane, B. R., and Dawson, J. H. (2010) Magnetic circular dichroism spectroscopic characterization of the nos-like protein from geobacillus stearothermophilus (gsnos), *J. Inorg. Biochem.* *104*, 357.
18. Tejero, J. S., Biswas, A., Wang, Z. Q., Page, R. C., Haque, M. M., Hemann, C., Zweier, J. L., Misra, S., and Stuehr, D. J. (2008) Stabilization and characterization of a heme-oxy reaction intermediate in inducible nitric-oxide synthase, *J. Biol. Chem.* *283*, 33498.
19. Hurshman, A. R., and Marletta, M. A. (1995) Nitric-oxide complexes of inducible nitric-oxide synthase - spectral characterization and effect on catalytic activity, *Biochemistry* *34*, 5627.
20. Nguyen, Y. H. L., Winkler, J. R., and Gray, H. B. (2007) Probing heme coordination states of inducible nitric oxide synthase with a re(i)(imidazole-alkyl-nitroarginine) sensitizer-wire, *J. Phys. Chem. B* *111*, 6628.
21. Agapie, T., Suseno, S., Woodward, J. J., Stoll, S., Britt, R. D., and Marletta, M. A. (2009) No formation by a catalytically self-sufficient bacterial nitric oxide synthase from sorangium cellulosum, *P. Natl. Acad. Sci. USA* *106*, 16221.
22. Zhu, Y. Q., and Silverman, R. B. (2008) Revisiting heme mechanisms. A perspective on the mechanisms of nitric oxide synthase (nos), heme oxygenase (ho), and cytochrome p450s (cyp450s), *Biochemistry* *47*, 2231.
23. Rittle, J., and Green, M. T. (2010) Cytochrome p450 compound i: Capture, characterization, and c-h bond activation kinetics, *Science* *330*, 933.
24. Tao, Z., Goodisman, J., and Souid, A.-K. (2008) Oxygen measurement via phosphorescence: Reaction of sodium dithionite with dissolved oxygen, *The Journal of Physical Chemistry A* *112*, 1511.
25. Wang, Z. Q., Wei, C. C., Sharma, M., Pant, K., Crane, B. R., and Stuehr, D. J. (2004) A conserved val to ile switch near the heme pocket of animal and bacterial nitric-oxide synthases helps determine their distinct catalytic profiles, *J. Biol. Chem.* *279*, 19018.
26. Presta, A., Weber-Main, A. M., Stankovich, M. T., and Stuehr, D. J. (1998) Comparative effects of substrates and pterin cofactor on the heme midpoint potential in inducible and neuronal nitric oxide synthases, *J. Am. Chem. Soc.* *120*, 9460.
27. Wei, C. C., Wang, Z. Q., Hemann, C., Hille, R., and Stuehr, D. J. (2003) A tetrahydrobiopterin radical forms and then becomes reduced during n-omega-hydroxyarginine oxidation by nitric-oxide synthase, *J. Biol. Chem.* *278*, 46668.